IJIREEICE

ISSN (Online) 2321-2004
ISSN (Print) 2321-5526

International Journal of Innovative Research in
Electrical, Electronics, Instrumentation and Control Engineering

Vol. 9, Issue 5, May 2021

DOI 10.17148/IJIREEICE.2021.9511

THREE PORT SWITCHING CONVERTER FOR HYBRID SOFT APPLICATIONS

M.Raja[1], G.Balaji[2],S.Rathinavel[3*] M.Arivazhagan[4], R.Dhanraj[5], A.Dileepan[6],G.Karthikeyan[7]

Assistant Professor, Department of Electrical and Electronics Engineering, Paavai Engineering College (Autonomous), Namakkal - 637 018, Tamilnadu, India[1,2,3]

Students, Department of Electrical and Electronics Engineering, Paavai Engineering College (Autonomous), Namakkal - 637 018, Tamilnadu, India[4,5,6,7]

Abstract: A comprehensive mathematical modeling and control design for an isolated multi-port DC/DC converter for photovoltaic (PV) generation systems is discussed in this paper. The adopted converter is a modified flyback converter consisting of three ports, namely, a photovoltaic (PV) module input port, a bi-directional battery port, and an isolated output port. The output port is receiving its demanded power without any interruption, while the power extracted from the PV module is maximized adopting a maximum power point tracking (MPPT) controller. Moreover, to improve the overall efficiency of the system, synchronous rectification switches are used on the secondary side of the isolation transformer. Set of simulations using MATLAB/Simulink are done to show the effectiveness of the proposed converter under different operating conditions.

Keywords: Congestion management, Deregulated Electricity market, Transmission Congestion Distribution Factor.

1.INTRODUCTION

TRADITIONAL DC-DC CONVERTER

Renewable sources such as solar photovoltaic (PV) and wind are increasingly being used because of the environmental concern and advances in the technology and rapidly decreasing manufacturing cost. However, the intermittent nature of the renewable sources and the unpredictability of the load demand produce a challenge for the wide promotion of these clean energy sources. Therefore, power electronic converters with energy storage systems are usually used to convert the output power from the PV panels to match the load demand, to improve the dynamic and steady-state characteristics of the green generation systems, to provide MPPT control, and to integrate the energy storage system to deal with the challenge of the intermittent nature of the renewable energy and the unpredictability of the load demand.

Traditionally, the renewable energy source is connected to the load through a traditional DC-DC converter and then the energy storage system is connected to either the input port or the output port of the traditional DC-DC converter through a bidirectional DCDC converter for charging and discharging as shown in Fig. 1.1 (a) and Fig. 1.1 (b). The main disadvantage of these traditional solutions is the low efficiency due to the utilization of the additional converter for the energy storage system. Also, the multi-stage architecture may result in increased size, low power density, and relatively high cost.

A multi-input converter is a solution to satisfy the requirements of some applications that require the integration of several different types of input energy sources such as fuel cells, wind turbines, and solar PV [9]. This type of converter can be used to provide the demanded power of the load with a single stage technique; however, no energy storage system is included in these multi-input converters, and hence the system may not be able to meet the required load demand when the output power is greater than the input power. For fuel cell operation, this may happen when there is a sudden increase in load and the chemical reaction of the fuel cell is not fast enough to follow the increase in load. Similarly for solar PV application, there may be fast PV output fluctuation during passing cloud causing the PV output to be less than the load demand or when there is no sun irradiation at night. Wind power output also fluctuates with the wind speed variation.

IJIREEICE

ISSN (Online) 2321-2004
ISSN (Print) 2321-5526

International Journal of Innovative Research in
Electrical, Electronics, Instrumentation and Control Engineering

Vol. 9, Issue 5, May 2021

DOI 10.17148/IJIREEICE.2021.9511

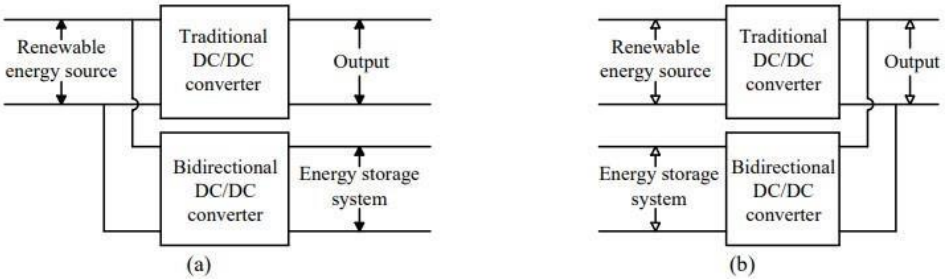

Fig. 1.1 Traditional power electronic systems in renewable energy system, (a) type 1, (b) type 2

Recently, the three-port DC-DC converters with the configuration shown in Fig.1.1.1 have been studied to integrate the renewable energy and energy storage converters into one converter with two inputs. One three-port DC-DC converter can accept two inputs: one input is for the DC output of the PV, and the second DC input, which is a bidirectional port, is for the energy storage system for charging and discharging. The output of the threeport DC-DC converter can be connected to the DC load directly or to the grid or AC load by an inverter through a DC link capacitor. Many three-port DC-DC converters, which can satisfy the MPPT and energy-storage charging and discharging requirement, have been reported in the literature. These converters can be categorized into 3 types: non-isolated, partly-isolated, and isolated converters.

Also, the use of a transformer may make the converter bulky and reduce Nonisolated three-port converters can result in reduced components numbers and a compact structure. Also, a systematic method of the derivation of non -isolated three-port converters. Compared to the non-isolated three-port converters, partly-isolated three-port converters, which use a transformer to isolate one port from the other two common grounded ports, can obtain higher voltage gain with a larger turn's ratio of the transformer. and modulation methods, high power loss may still occur due to the leakage inductance of the transformer. Since all of the three ports are connected directly, this type of converter can only be used in those applications where the galvanic insulation is not required. Another disadvantage of the non-isolated three-port converters is that most of these converters have a limited voltage gain since the freedom of modulation of the voltage conversion ratio is only the duty cycle.

Some reported papers use coupled-inductor to extend the voltage conversion ratio to overcome this issue

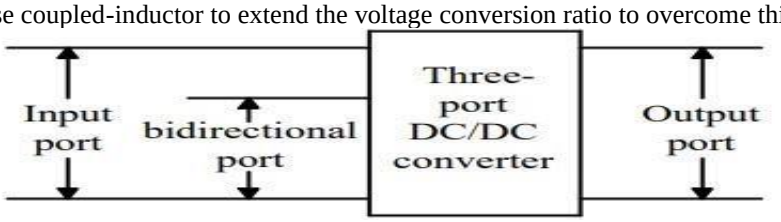

Fig. 1.1.1 The typical structure of three-port converter

However, the energy storage system in these converters continues operating in all operating modes, which can shorten the lifespan of the energy system and lower the reliability of the overall system. Similar to the partly-isolated converters, the isolated converters are based on the use of a high-frequency transformer, which can help them to well balance the different voltage levels among the different ports. However, the number of the components used in this kind of converter is very large since the components are seldom shared. Although both of the partly-isolated and isolated converters can be operated with soft switching on the switches using appropriate control the overall power density.

THE GENERAL OPERATING PRINCIPLES OF A DC-DC THREEPORT CONVERTER

For a traditional two-port DC-DC power electronic converter, the main function is to implement the energy conversion between the two ports. In fact, all of the multi-port DCDC converters can be viewed as the combination of several two port DC-DC converters and the function of these new converters is to implement a simplified topology for the energy conversion between any two of all the ports available in the converter.

It can be seen that the DC input port of the converter is connected to the DC output of the renewable source; the DC bidirectional port is connected to the DC energy storage system and the DC output port is connected to the DC load. In term of the power-balance principle, the relationship of the powers among the three ports can be expressed as:

$$Pin + Pb = Po \; . \quad (1)$$

where P_{in} is the DC input power, P_b is the DC bidirectional power and P_o is the DC output power.

IJIREEICE

ISSN (Online) 2321-2004
ISSN (Print) 2321-5526

International Journal of Innovative Research in
Electrical, Electronics, Instrumentation and Control Engineering

Vol. 9, Issue 5, May 2021

DOI 10.17148/IJIREEICE.2021.9511

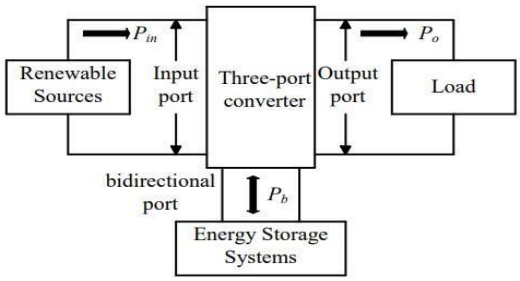

Fig.1.2. The general configuration of a renewable energy generation system using a three-port converter

Since the DC input power can be either higher or lower than the DC output power (load demand), the three-port DCDC converter has three operation modes, which are described as follows:
When the DC input power is higher than the DC output power, the three-port DCDC converter will operate under single-input dual-output (SIDO) mode, which means that only the renewable source is the input source and the energy storage system can be viewed as an additional load. The input source will supply the load alone and charge the energy storage system using the surplus power. The equivalent expression of the power flow in the converter during this operation mode is shown in Fig. 1.2.1 (a).
When the DC input power is lower than the DC output power, the three-port DC-DC converter will operate under dual-input single-output (DISO) mode, which means that the energy storage system is an additional input source. The equivalent expression of the power flow in the converter during this operation mode is shown in Fig. 1.2.1 (b).
When the DC input power is not available or the DC input power is zero, the threeport DC-DC converter will operate under single-input single-output (SISO) mode, which is similar to the traditional DC-DC two-port converter. During this mode, the energy storage system will be discharged to supply the load alone. The equivalent expression of the power flow in the converter during this operation mode is shown in Fig. 1.2.1 (c).

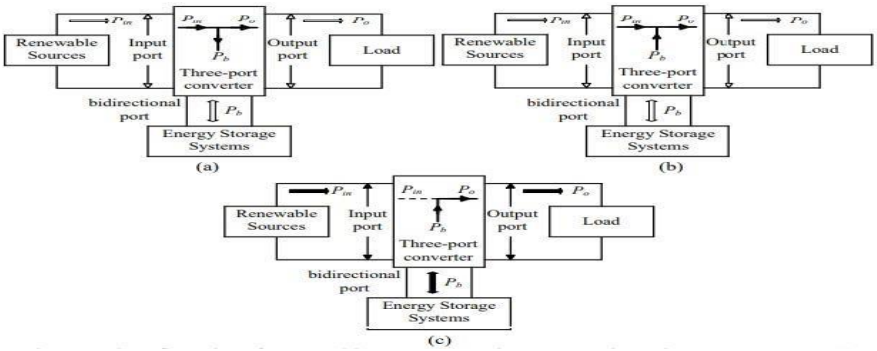

Fig. 1.2.1. The general configuration of a renewable energy generation system using a three-port converter, (a) SIDO mode, (b) DISO mode, (c) SISO mode

REPORTED THREE-PORT DC-DC CONVERTERS

As mentioned previously, many three-port DC-DC converters have been proposed recently. They have the advantages of higher efficiency and higher power density. These converters are preferable candidates for solving the issues that are produced by the intermittent nature of the renewable sources and the unpredictability of the load demand, by incorporating energy storage as an additional DC input. Depending on the connection among the three ports, this kind of converters can be classified into three types: (i) non-isolated three-port DC-DC converters, (ii) partlyisolated DC-DC three-port converters, and (iii) isolated three-port DC-DC converters. The configuration of the non-isolated three-port DCDC converters, which shows that all of the three ports of the converter are connected directly without any galvanic isolation, which can result in small size and high power density. Both partly-isolated and isolated converters use a high-frequency transformer to implement the isolation between different ports to avoid shock hazards. Another function of the transformer is to extend the voltage conversion ratio of the converter. However, when compared with the non-isolated converters, the use of the high-frequency transformer will increase the overall size and therefore relatively reduce the power density and efficiency of the converter. Along with appropriate PWM modulation methods and power management strategies, these three types of converters can be implemented to satisfy the requirements of particular industrial applications.

IJIREEICE

ISSN (Online) 2321-2004
ISSN (Print) 2321-5526

International Journal of Innovative Research in
Electrical, Electronics, Instrumentation and Control Engineering

Vol. 9, Issue 5, May 2021

DOI 10.17148/IJIREEICE.2021.9511

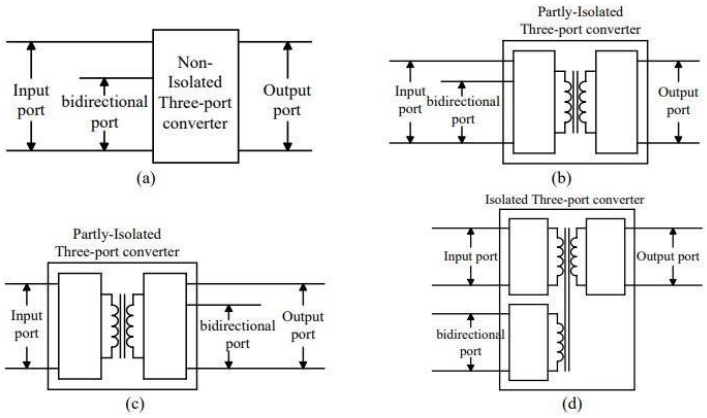

Fig.1.3. The typical structure of three-port converter, (a) non-isolated, (b) partly- isolated type 1, (c) partly-isolated type 2, (d) isolated

Non-Isolated Three-Port DC-DC Converters

Since most of these converters are derived based on the traditional boost, buck, buckboost converters, the gain of these converters are limited. To overcome limitation, some three-port DC-DC converters use coupled inductors to extend the voltage conversion ratio.

A novel non-isolated three-port converter by combining a traditional boost converter and a buck converter together using an additional switch as shown in Fig. 1.3.1.1.

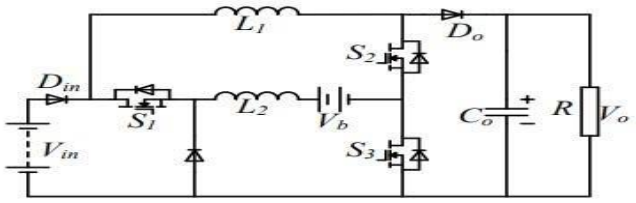

Fig.1.3.1.1. A novel non-isolated three-port converter by combining a traditional boost converter and a buck converter together using an additional switch

By combining any two of the three basic converters (buck,boost,and buck boost converter), a family of novel two inductor three-port DC-DC converters. These converters use only one switch to manage the power distribution among the three ports, which reduces the size and cost of the converter.

A new three-port DC-DC converter with a high voltage conversion ratio is proposed as shown in Fig. 1. Although the voltage gain is extended and the voltage stresses of the input side switches are reduced through the utilization of two coupled-inductors, the structure of this converter is relatively complex, since five switches are required, increasing the cost of the converter. However, one advantage of this converter is the high efficiency due to the use of active clamped circuits that can recycle the energy stored in the leakage inductors.

Based on the converter, a novel high step-up three-port DC-DC converter as shown in Fig. 1.3.1.2. By applying the coupled inductor and switched-capacitor circuits the output port of the converter shown in Fig.1.3.1.2, the obtained converter can achieve a much higher voltage conversion ratio using a reasonable duty cycle and an appropriate turn ratio of the coupled-inductor when compared with the converter. Therefore, regulating freedom of the duty cycle is enlarged.

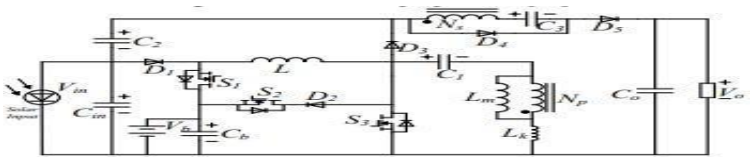

Fig.1.3.1.2. A novel high step-up three-port DC-DC converter

A three-port DC-DC converter with high voltage conversion ratio, based on a unidirectional three-state switching cell as shown in Fig. 1.3.1.5. Due to the natural characteristics of the structure of this converter, all of the switches can operate

IJIREEICE

ISSN (Online) 2321-2004
ISSN (Print) 2321-5526

International Journal of Innovative Research in
Electrical, Electronics, Instrumentation and Control Engineering

Vol. 9, Issue 5, May 2021

DOI 10.17148/IJIREEICE.2021.9511

under the soft switching condition over a wide operation range and with reduced voltage stresses, which can result in a high overall efficiency. The features such as high-gain, high efficiency and soft switching of the converter are validated by a 500W prototype in the laboratory as reported in [23].

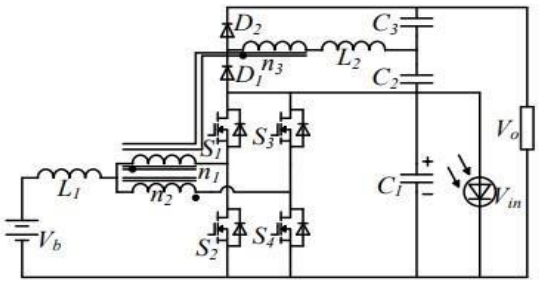

Fig.1.3.1.5. A three-port DC-DC converter with high voltage conversion ratio based on a unidirectional three-state switching cell

2.PARTLY-ISOLATED THREE-PORT DC-DC CONVERTERS

Partly-isolated three-port DC-DC converters usually have two of the three ports connected directly, and then these ports are connected to the third port with galvanic isolation. Most of these types of converters usually have the input port and the bidirectional port connected directly and then they are connected to the isolated output port as shown in Fig.1.3(b).There are also other partly-isolated three-port converters that have the output port and the bidirectional port connected without any galvanic isolation but these ports are then connected to the input port through a high frequency transformer as shown in Fig. 1.3 (c).

A three-port DC-DC converter based on the half-bridge converter is proposed and analysed in [25] and [26] as shown in Fig. 1.3.2.1. The proposed converter is derived from the traditional half-bridge converter by applying an additional switch and a diode in the primary side of the transformer and using two switches to replace the diode in the output port. All the switches in the primary side can operate under zero voltage switching for a wide range of operation conditions. The power flow among the three ports can be controlled by controlling the duty cycles of the two primary-side switches. The application of this converter using appropriate modulation techniques and power management strategies. The efficiency of these converters is relatively high as the power flow between any two of the three ports is in single stage. Since there are two switches in the secondary side of the transformer for synchronous regulation, the voltage of the three ports can be regulated independently.

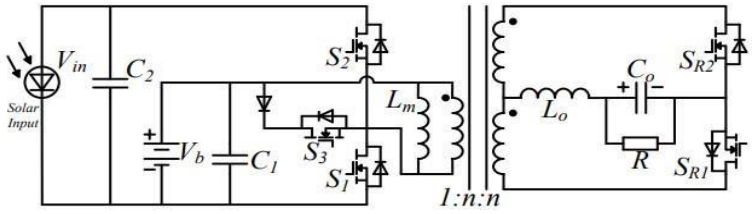

Fig.1.3.2.1. A three-port DC-DC converter based on the half-bridge converter

A novel partly-isolated three-port DC-DC converter derived from half-bridge converter for a stand-alone renewable power system application as shown in Fig. 1.3.2.2. By applying a post-regulation to replace the synchronous regulation in the converter, several other converters can be derived. All of the obtained converters have advantages of reduced number of components and relatively simple configurations. This converter has been modularized and integrated to build DC distribution power system with a system level power management technique.

By combining two buck-boost converters and a full-bridge switching cell, a new three-port DC-DC converter as shown in Fig.1.3.2.4. Similar to this converter, another two converters, which have the similar structure as this converter in the primary side of the transformer but different structure in the secondary side, as shown in Figs.1.3.2.2 – 1.3.2.3. Following the same concept, a three phase three-port DC-DC converter as shown in Fig. 23 for PV application in a DC distribution system.

IJIREEICE

ISSN (Online) 2321-2004
ISSN (Print) 2321-5526

International Journal of Innovative Research in
Electrical, Electronics, Instrumentation and Control Engineering

Vol. 9, Issue 5, May 2021

DOI 10.17148/IJIREEICE.2021.9511

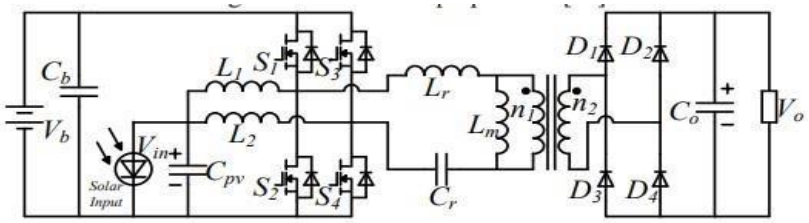

Fig.1.3.2.2 By combining two buck-boost converters and a full-bridge switching cell, a new three-port DC-DC converter by battery

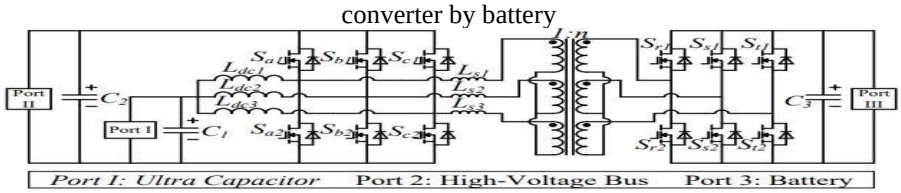

Fig.1.3.2.3 A three phase three port DC-DC converter

Based on an improved Flyback-Forward converter, a new partly-isolated three-port DC-DC converter as shown in Fig. 1.3.2.9 for standalone PV systems. When the PV supplies the load and the battery, the switches S_1 and S_2 operates with the same duty cycles with an 180^o phase displacement, while the switches S_3 and S_4 operate under synchronously rectifying mode. When the battery supplies the load alone, the converter functions as the traditional flyback-forward converter, which means that the switches S_3 and S_4 are the main switches, and the other two switches are used to form the active clamp circuits. When the PV charges the battery and the load is disconnected, the proposed converter can be viewed as two independently buck-boost converters connected in parallel. Another two partly isolated converters, which are based on the flyback converter, as shown in Fig. 1.3.2.4 and Fig. 1.3.2.5 respectively.

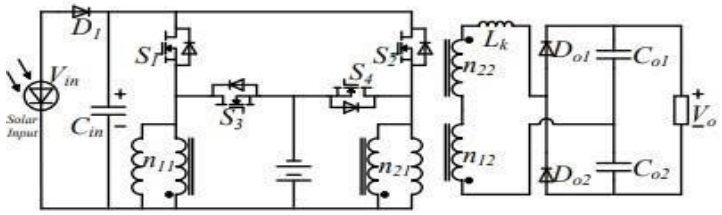

Fig 1.3.2.4. Based on an improved Fly Back-Forward converter, a new partly isolated three-port DC-DC converter

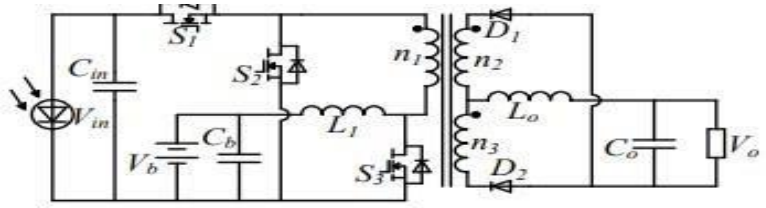

Fig 1.3.2.5. Two independently buck-boost converters connected in parallel

Different from the above presented converters, which integrate the input port and the bidirectional port to the primary side of the high-frequency transformer, a novel partlyisolated converter, which integrates the bidirectional port and the load to the secondary side of the transformer and the PV is isolated at the primary side of the transformer, as shown in Fig. 1.3.3.1. The detailed derivation of the proposed converter from the traditional half-bridge converter. The output circuit of the traditional half-bridge converter is detached first and then a boost converter is inserted between the two detached outputs to provide the power flow path between the battery and the load

IJIREEICE

ISSN (Online) 2321-2004
ISSN (Print) 2321-5526

International Journal of Innovative Research in
Electrical, Electronics, Instrumentation and Control Engineering

Vol. 9, Issue 5, May 2021

DOI 10.17148/IJIREEICE.2021.9511

3.ISOLATED THREE-PORT DC-DC CONVERTERS

An isolated three-port DC-DC converter based on the combination of a three fullbridge structure and a three-winding transformer, as shown in Fig.1.3.3.2. Although it was proposed for the hybrid fuel cell system application, it can be used in other renewable energy applications such as PV generation systems. After the introduction of this converter, it has gained a lot of attention from other researchers, in terms of the analysis of the performances of the converter, the control methods, the loss evaluations, and its applications. In order to reduce the ripples of the input current, an inductor has been added between the input source and the full-bridge structure in the input port as shown in Fig.1.3.3.3. Compared to the converter shown in Fig. 1.3.3.2, this converter includes two additional series resonant circuit in the primary side of the transformer, to implement the soft switching of the switches to reduce the switching losses. Another benefit of this converter over the previous one is that this converter can operate with a high switching frequency with realizable component values. The full-bridge circuit and half bridge circuit can also be combined to implement an isolated three-port DC-DC converter as reported in [60]. The obtained converter is shown in Fig. 1.3.3.3.

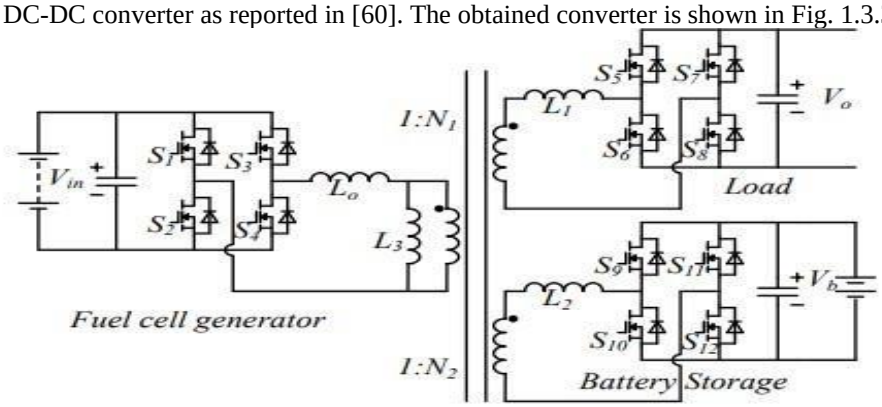

Fig 1.3.3.1 An isolated three-port DC-DC converter based on the combination of a three full-bridge structure and a three-winding transformer

.

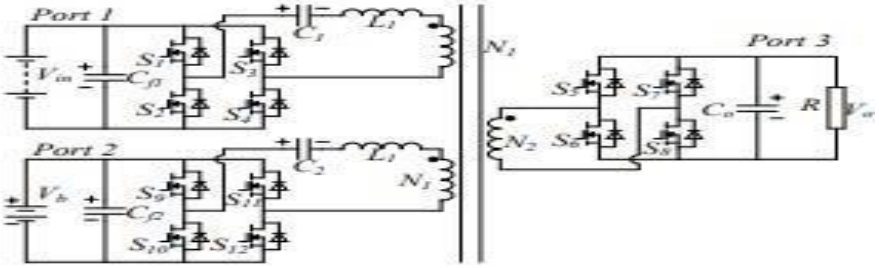

Fig 1.3.3.2 A new full-bridge based three-port DC-DC converter

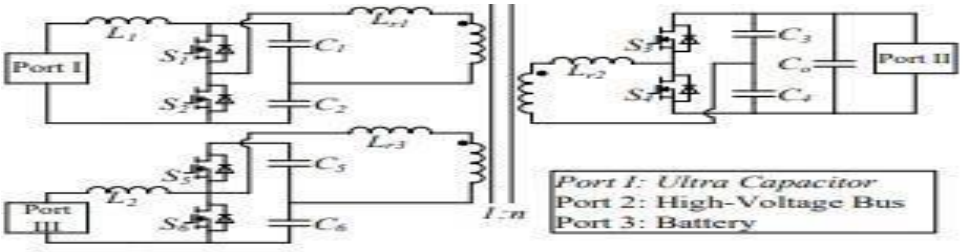

Fig 1.3.3.3 A new three-port DC-DC converter with additional inductor

IJIREEICE

ISSN (Online) 2321-2004
ISSN (Print) 2321-5526

International Journal of Innovative Research in
Electrical, Electronics, Instrumentation and Control Engineering

Vol. 9, Issue 5, May 2021

DOI 10.17148/IJIREEICE.2021.9511

4.CONFIGURATION OF AN ISOLATED MULTI-PORT DC/DC CONVERTER

Although renewable energy resources are sustainable and clean, their integration in the network puts some challenges to be faced in order to harness them effectively [1, 2]. In [3], a detailed study regarding the impact of different power electronics converters on the performance improvement of renewable energy harnessing is discussed.

Photovoltaic (PV) generation systems will be investigated. The DC/DC converters are one of the main and essential apparatuses in this integrating process that affect the overall performance of PV generation systems [3 b].

Recently, different converter topologies have been proposed to achieve a high stepup conversion ratio, such as series boost converters [6], the voltage-lift technique [7], and a coupled inductor [9-11]. In [9] a high step-up DC/DC coupled inductor converter, such that, the extreme duty ratio is eliminated and rectifier reverse-recovery problem is solved, but coupled inductor converter requires high-current stress power components, due to the large current that flows through them, that indicates higher cost and less efficient system.

These converters can be categorized into different types such as, non-isolated and isolated converters [16-20]. Based on single-ended primary-inductor multiplier and a Buck Boost Converters a three-port non-isolated DC/DC converter for DC micro grid application was proposed in [18]. However, this type of the multi-port DC/DC converter can only be used in applications where the galvanic insulation is not required, and in general, most of the non-isolated three-port converters have a limited voltage gain that depends only on duty cycle [20].

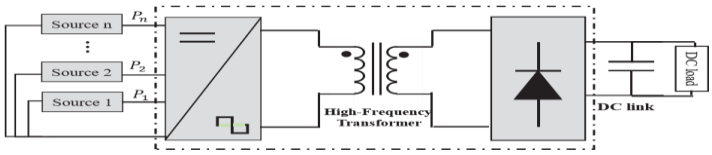

Fig 4.1 Configuration of an isolated multi-port DC/DC converter

An isolated three-port DC/DC converter was proposed in [21], but synchronous rectification switches may be used to improve the system efficiency. In [22] an improved isolated bi-directional flyback DC/DC converter is proposed, it combines the advantages of both the bi-directional converter and the three-port converter with a reduction in cost and size, but it has only one independent control signal. Reference [24] proposed an isolated three-port DC/DC converter with synchronous rectification switches to improve system efficiency with its control strategies based on small-signal model.

In this paper, a multi-port isolated DC/DC converter is proposed with its modeling and control design. The controllers' design will be carried out based on the system smallsignal model that is built based on a comprehensive mathematical modeling of the proposed converter considering the parasitic elements.

PWM GENERATOR

The PWM Generator block generates pulses for carrier-based pulse width modulation converters using two-level topology. The block can be used to fire the forced-commutated devices of single-phase,two phase, three-phase or a combination of two three-phase bridges.

✓ SG3525 is a pulse width modulated control circuit that is used to control switching power supplies and particularly helps in providing lower external parts count and improved performance.

✓ It is voltage control PWM controller in which feedback voltage is compared with reference value which then controls the duty cycle of PWM.

✓ It is mainly used in inverter applications and utilizes two main PWM outputs that are inversion of each other.

✓ The on-chip +5.1 references is modified to ±1% and the error amplifier that comes with both input common mode voltage range and reference voltage, helps in terminating the need of external resistors.

✓ A sync input provided to the oscillator helps in synchronizing single unit to the external system clock.

✓ A single resistor existed between the discharge pins and Ct is used to program the wide range of dead time.

✓ This modulator is also incorporated with built-in-soft start-circuitry which needs external timing capacitor.

✓ A shutdown pin is used to control both output stages and soft-start circuitry that also features instantaneous turn-off with the help of PWM latch and pulsed shutdown.

✓ When Vcc stays below nominal, the under voltage lockout limits both soft-start capacitor and outputs.

PIN DESCRIPTION

- SG3525 is a 16 pin IC. Each pin is allocated with different function.
- Following figure shows the pin number, pin name and functions associated with each pin.
- Soft start and compensation terminals receive the pull down signal and turn off the outputs when it sinks a maximum of 100µA current.

IJIREEICE

ISSN (Online) 2321-2004
ISSN (Print) 2321-5526

International Journal of Innovative Research in
Electrical, Electronics, Instrumentation and Control Engineering

Vol. 9, Issue 5, May 2021

DOI 10.17148/IJIREEICE.2021.9511

- There is another way of turning off the output which involves the shutdown circuitry of pin 10 that comes with an added amount of shutdown options.
- This circuit is activated by providing positive signal at the pin 10 which then executes two functions i.e. output signal turns off by immediately setting PWM latch and soft-start capacitor starts to discharge during the availability of 150 µA current.
- If the shutdown command is applied for short period of time, the PWM signal will be eliminated without discharging soft-start capacitor significantly helps in carrying out pulse by pulse current limiting.
- However, if pin 10 is hold for longer duration will discharge the external capacitor quickly.

FEATURES

- 5.1V ± 1.0% Trimmed Reference
- 8V to 35V Operation
- Separate Oscillator Sync Pin
- 100 Hz to 400 kHz Oscillator Range
- Input Under voltage Lockout
- Adjustable Dead time Control
- Pulse-by-Pulse Shutdown
- Dual Source/Sink Outputs
- Latching PWM to Prevent Multiple Pulses

PINOUT

- Pinout diagram features proper and detailed configuration of any electronic device.
- SG3525 pinout diagram is shown in the figure below which elaborates the configuration of each pin of this modulator.
- Block diagram is described in schematic form which features the general arrangement of parts or elements used in the device or process.
- Following figure shows the block diagram of SG3525.
- It is clear from the figure that output stage of this modulator represents NOR logic.

VOLTAGE CONTROLLER

Voltage Controller is employed to vary the RMS value of the alternating voltage applied to a load circuit by introducing Thyristors between the load and constant voltage ac source. The RMS value of alternating voltage applied to a load circuit is controlled the triggering angel of the thyristors in the voltage controller circuits. In brief, a Voltae Controller is a type of thyristor power converter which is used to convert a fixed voltage, fixed frequency ac input supply to obtain a variable ac output. The RMS value of the ac output voltage and the ac power flow to the load is controlled by varying the trigger angle ‘α’.

RECTIFIER

A Rectifier is an electrical device composed of one or more diodes that converts alternating current (AC) to direct current (DC). A diode is like a one-way valve that allows an electrical current to flow in only one direcion. This process is called rectification. A rectifier can take the shpae of several different physical forms such as solid-state diodes, vaccum tube diodes, mercury arc valves, silicon-controlled rectifiers and various other silicon-based semiconductor switches. Rectifiers have many uses, but are often found serving as components of DC power supplies and high-voltage direct current power transmisiion systems.

Depending on the type of alternating current supply and the arrangement of the rectifier circuit, the output voltage may require additional smoothing to produce a uniform steady voltage. Many applications of rectifiers, such as power supplies for radio, television and computer equipment, require a steady constant DC voltage. In these applications the output of the rectifer is smoothed by an electronic filter, which may be a capacitor, choke, a set of capacitors, possibly followed by a voltage regulator to produce a steady voltage. The primary application of rectifiers is to derive DC power from an AC supply. Rectifiers are used inside the power supplies of virtually all electronic equipment. In such power supplies, the rectifier will be in series following the transformer, and be followed by a smoothing filter and possibly a voltage regulator.

PIC MICRO CONTROLLER

PIC16F877A

PIC is a family of modified Harvard architecture microcontrollers made by Microchip Technology, derived from the PIC1650 originally developed by General Instrument’s Microelectronics Division. The name PIC initially referred to “Peripheral Interface Controller”. PICs are popular with both industrial developers and hobbyists alike due to their low

IJIREEICE

ISSN (Online) 2321-2004
ISSN (Print) 2321-5526

International Journal of Innovative Research in
Electrical, Electronics, Instrumentation and Control Engineering

Vol. 9, Issue 5, May 2021

DOI 10.17148/IJIREEICE.2021.9511

cost, wide availability, large user base, extensive collection of application notes, availability of low cost or free development tools, and serial programming (and re-programming with flash memory) capability.

HIGH PERFORMANCE RISC CPU

PIC has only 35 single word instructions. All are single cycle instructions except for program branches, which uses two-cycle. The Operating speed of PIC in DC is 20 MHz and clock input in DC is 200 ns instruction cycle. The PIC has 8K x 14 words of flash Program Memory, 368 x 8 bytes of Data Memory (RAM).

PERIPHERAL FEATURES

- Timer0: 8-bit timer/counter with 8-bit presales.
- Timer1: 16-bit timer/counter with presales.
- Timer2:8-bit timer/counter with 8-bit period register, presales and post sales.
- It has a Capture, Compare, PWM (CCP) module. Capture is of 16-bit and it has a maximum resolution of 12.5 ns. Compare is of 16-bit and it has a maximum resolution of 200ns.Pulse Width Modulation has a maximum resolution of 10-bit.8-bit,
- 8 channel analog-to-digital converter with 10 bit each.
- It has a Synchronous Serial Port (SSP) with SPI (Master/Slave) and I2C, USART with 9 bit detection. It also has a Brown-out detection circuitry for Brown-out Reset (BOR).

CMOS TECHNOLOGY

PIC has a Low power, high speed CMOS FLASH technologywith a fully static design**.** It provides a wide operating voltage range of 2.0V to 5.5V.It has Low power consumption and used in commercial and industrial temperature ranges.

PIN DIAGRAM

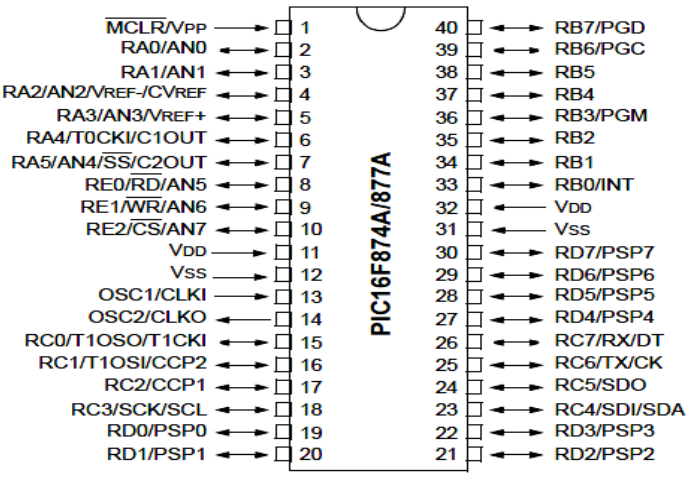

Fig.4.2.1. Pin Diagram of Pic16f877a

MEMORY ORGANIZATION

There are three memory blocks in the PIC16F87XA device. The program memory and the data memory have separate buses so that concurrent access can occur. The PIC16F87XA devices have 13 bit program counter capable of addressing an 8K x 14 bit program memory space. The data memory is partitioned into multiple banks which contain the general purpose registers and the Special Function Registers (SFRs). Bits RP1 and RP0 are the bank select bits.

IJIREEICE

ISSN (Online) 2321-2004
ISSN (Print) 2321-5526

International Journal of Innovative Research in
Electrical, Electronics, Instrumentation and Control Engineering

Vol. 9, Issue 5, May 2021

DOI 10.17148/IJIREEICE.2021.9511

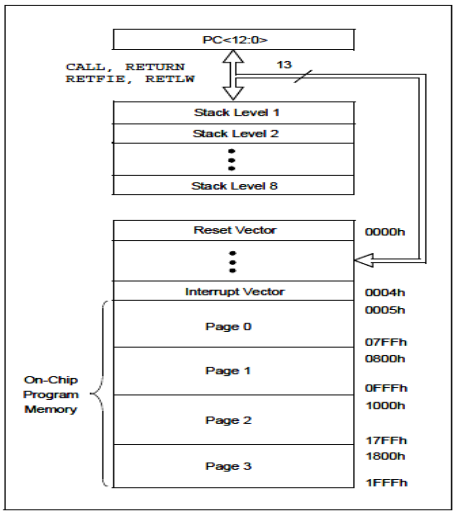

Fig.4.2.2. Program Memory Organization and Stack

I/O PORTS

I/O ports are multiplexed with an alternate function for the peripheral features on the device. In general, when a peripheral is enabled, that pin may not be used as a general purpose I/O pin.

PORTA AND THE TRISA REGISTER

PORTA is a 6-bit wide, bidirectional port. The corresponding data direction register is TRISA. Setting a TRISA bit (= 1) will make the corresponding PORTA pin an input (i.e., put the corresponding output driver in a High-Impedance mode). Clearing a TRISA bit (= 0) will make the corresponding PORTA pin an output (i.e., put the contents of the output latch on the selected pin).

PORTB AND THE TRISB REGISTER

PORTB is an 8-bit wide, bidirectional port. The corresponding data direction registers isTRISB. Setting a TRISB bit (= 1) will make the corresponding PORTB pin an input (i.e., put the corresponding output driver in a High-Impedance mode). Clearing a TRISB bit (= 0) will make the corresponding PORTB pin an output (i.e., put the contents of the output latch on the selected pin).

PORTC AND THE TRISC REGISTER

PORTC is an 8-bit wide, bidirectional port. The corresponding data direction register is TRISC. Setting aTRISC bit (= 1) will make the corresponding PORTC pin an input (i.e., put the corresponding output driver in a High-Impedance mode). Clearing a TRISC bit (= 0) will make the corresponding PORTC pin an output (i.e., put the contents of the output latch on the selected pin).

PORTD AND THE TRISD REGISTER

PORTD is an 8-bit port with Schmitt Trigger input buffers. Each pin is individually configurable as an input or output. PORTD can be configured as an 8-bit wide microprocessor port (Parallel Slave Port) by setting control bit, PSPMODE (TRISE<4>). In this mode, the input buffers are TTL.

PORTE AND TRISE REGISTER

PORTE has three pins (RE0/RD/AN5, RE1/WR/AN6and RE2/CS/AN7) which are individually configurable as inputs or outputs. These pins have Schmitt Trigger input buffers. The PORTE pins become the I/O control inputs for the microprocessor port when bit PSPMODE (TRISE<4>) is set. In this mode, the user must make certain that the TRISE<2:0> bits are set and that the pins are configured as digital inputs. Also, ensure that ADCON1 is configured for digital I/O. In this mode, the input buffers are TTL.

PIC C COMPILER

CCS provides a method to attempt to make sure you can compile code written in older versions of CCSwith minimal difficulty by altering the methodology to best match the desired version. Currently, thereare 4 levels of compatibility provided: CCS V2.XXX, CCS V3.XXX, CCS V4.XXX and ANSI.

IJIREEICE

ISSN (Online) 2321-2004
ISSN (Print) 2321-5526

International Journal of Innovative Research in
Electrical, Electronics, Instrumentation and Control Engineering

Vol. 9, Issue 5, May 2021

DOI 10.17148/IJIREEICE.2021.9511

Notice: this only affects the compiler methodology, it does not change any drivers, libraries and includefiles that may have been available in previous versions.

#device CCS2

• ADC default size is set to the resolution of the device (#device ADC=10, #device ADC=12, etc)
• boolean = int8 is compiled as: boolean = (int8 != 0)
• Overload directive is required if you want to overload functions
• Pointer size was set to only access first bank (PCM *=8, PCB *=5)
• var16 = NegConst8 is compiled as: var16 = NegConst8 & 0xFF (no sign extension)
• Compiler will NOT automatically set certain #fuses based upon certain code conditions.
• rom qualifier is called _rom

#device CCS3

• ADC default is 8 bits (#device ADC=8)
• boolean = int8 is compiled as: boolean = (int8 & 1)
• Overload directive is required if you want to overload functions
• Pointer size was set to only access first bank (PCM *=8, PCB *=5)
• var16 = NegConst8 is compiled as: var16 = NegConst8 & 0xFF (no sign extension)
• Compiler will NOT automatically set certain #fuses based upon certain code conditions.
• rom qualifier is called _rom

#device CCS4

• ADC default is 8 bits (#device ADC=8)
• boolean = int8 is compiled as: boolean = (int8 & 1)
• You can overload functions without the overload directive
• If the device has more than one bank of RAM, the default pointer size is now 16 (#device *=16)
• var16 = NegConst8 is will perform the proper sign extension
• Automatic #fuses configuration (see next section)

#device ANSI

• Same as CCS4, but if there are any discrepancies are found that differ with the ANSI standard then the change will be made to ANSI
• Data is signed by default
• const qualifier is read-only RAM, not placed into program memory (use rom qualifier to place into program memory)
• Compilation is case sensitive by default
• Constant strings can be passed to functions (#device PASS_STRINGS_IN_RAM)

This C compiler, is fully optimised for use with PIC microcontrollers. Built in functions make coding the software very easy. Based on original K&R, the integrated C development environment gives developers a fast method to produce efficient code from an easily Maintainable high level language.

CAPABILITIES

· Arrays up to 5 subscripts
· Structures and Unions may be nested.
· Custom bit fields (1-8 bits) within structures.
· ENUMurated types,
· CONSTant variables, arrays and strings.
· Full function parameter support (any number).
· Some support for C++ reference parameters.

FEATURES

- Built in Libraries for RS232 serial I/O library, I/O, I2C, discrete I/Oand precision delays.
- Integrates with MPLAB and other simulators/emulators for source level debugging.
- Standard Hex file and debug files ensure compatibility with all programmers.
- Formatted Printf allows easy formatting and display in Hex or decimal.
- Efficient function implementation allows call trees deeper than the hardware stack.
- Access to hardware from easy to use C functions, Timers, A/D, E2, SSP, PSP, I2C & more.
- 1,8, and 16 bit types.
- Assembly code may be inserted anywhere in source and may reference C variables.

IJIREEICE

ISSN (Online) 2321-2004
ISSN (Print) 2321-5526

International Journal of Innovative Research in
Electrical, Electronics, Instrumentation and Control Engineering

Vol. 9, Issue 5, May 2021

DOI 10.17148/IJIREEICE.2021.9511

- Automatic linking handles multiple code pages.
- Inline procedures supported; Linker automatically determines optimum architecture or it can be manually specified.
- Compiler directives determine if tri-state registers are refreshed on every I/O
- Constants (including strings and arrays) are saved in program memory.
- Standard one bit type (Short Int) permits the compiler to generate efficient Bit oriented code.
- #BIT and #BYTE allow C variables to be placed at absolute addresses to map register to C variables.
- Reference parameters may be used to improve code readability and inline procedure efficiency.
- Both an Integrated editor/compiler and a cmd line compiler.
- Special windows show the RAM memory map, C/Assembly listing and the calling tree.
- Interrupt procedures supported on PCM. The compiler generates all startup and cleanup code as well as identifying the correct interrupt procedure to be called.
- Updates via modem for 30 days included.

THE PROPOSED MULTI-PORT DC/DC CONVERTER ANALYSIS, MODELING, AND CONTROL

Circuit and Topology

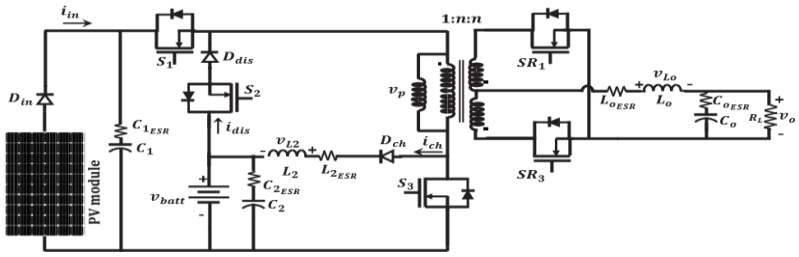

Fig 4.2. The proposed multi-port modified flyback converter.

Switch S1 is used to track the maximum power point of the PV module. The auxiliary inductor V_{12} in the battery charging path is used to provide a continuous battery charging current. Diode D_{dis} is used to prevent the PV module to be directly connected to the battery. Switch S_2 is used to control the discharging process of the battery when the available power from the PV is insufficient to cover the load power demand. Switch S_3 is used to regulate the output voltage. The synchronous rectification switches SR_1 and SR_2 are adopted rather than diodes to improve the overall system efficiency.

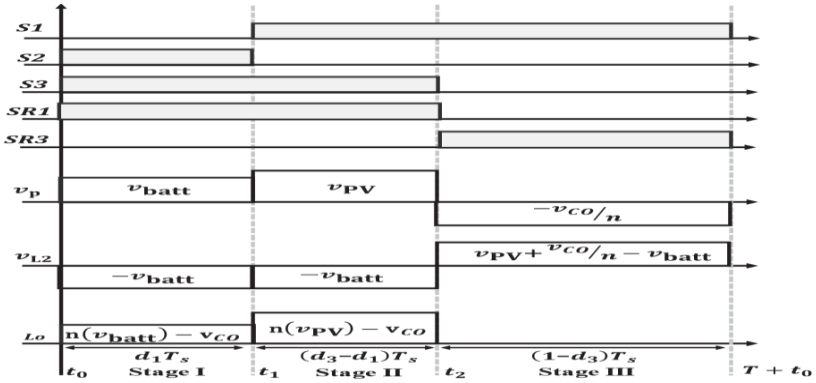

Fig 4.2.1. Basic waveforms of the proposed converter

Circuit Operation Principles

The steady-state waveforms of the proposed converter are shown in Fig. 4.2.1 It includes three basic converter stages within a constant-frequency switching cycle. This provides two independent control signals from duty cycles d1 and d2 which are needed to drive the switches S_1 and S_3, respectively. Switch S_2 should be turned on by the complement operation of the gate drive signal of the switch S_1 and the real gate drive signal of the switch S_3. SR_1 will be turned on when a positive voltage is applied at the primary side of the transformer, while SR_3 will be turned on when a negative voltage is applied.

IJIREEICE

ISSN (Online) 2321-2004
ISSN (Print) 2321-5526

International Journal of Innovative Research in
Electrical, Electronics, Instrumentation and Control Engineering

Vol. 9, Issue 5, May 2021

DOI 10.17148/IJIREEICE.2021.9511

Steady-State Analysis

Assume that the converter is lossless, the forward voltage conversion ratio can be determined using the volt-second balance equation across the converter main inductors, when the converter is operating in continuous conduction mode (CCM) by a proper selection of the inductor values above the discontinuous conduction mode (DCM) boundary. The volt-second balance equation across the auxiliary inductor L_2, can be written as:

$$v_{batt} = v_{PV}(1-d_3) + \frac{v_o}{n}(1-d_3) \qquad (1)$$

From the volt-second balance equation across the output inductor L_O, the forward voltage conversion ratio can be written as:

$$\frac{v_o}{v_{pv}} = n\frac{d_3(1-d_1)}{d_3-d_1+d_3d_1} \qquad (2)$$

MODELING AND CONTROL DESIGN

For the three-port converter which is a MIMO system, the traditional circuit averaging process can be used to carry out the system small-signal model analysis under different modes of operation. A decoupling network is then introduced to allow the separate controller designs for two ports of the system.

State Space Average Model

This stage is the discharge stage, and it will terminate when the switch S_1 is turned on. The state equations in this stage. The state equations in this stage are presented in Eq. (3).

$$\begin{cases} \frac{dv_{C1}}{dt} = \frac{1}{C_1}i_{C1} = \frac{1}{C_1}[i_{PV}] \\ \frac{dv_{C2}}{dt} = \frac{1}{C_2}i_{C2} = \frac{1}{C_2}\left[\frac{v_{batt}-v_{C2}}{C_{2ESR}} - ni_{Lo}\right] \\ \frac{di_{L2}}{dt} = \frac{1}{L_2}[-v_{batt} - i_{L2}L_{2ESR}] \\ \frac{di_{Lo}}{dt} = \frac{1}{L_o}\left[\begin{matrix} nv_{batt} - i_{Lo}L_{oESR} \\ -i_{Co}C_{oESR} - v_{Co} \end{matrix}\right] \\ \frac{dv_{Co}}{dt} = \frac{1}{C_o}i_{Co} = \frac{1}{C_o}\left[i_{Lo} - \frac{v_{Co}}{R_L+C_{oESR}}\right] \end{cases} \qquad (3)$$

The state equations in this stage are as in Eq. (4).

$$\begin{cases} \frac{dv_{C1}}{dt} = \frac{1}{C_1}i_{C1} = \frac{1}{C_1}[i_{PV} - ni_{Lo}] \\ \frac{dv_{C2}}{dt} = \frac{1}{C_2}i_{C2} = \frac{1}{C_2}\left[\frac{v_{batt}-v_{C2}}{C_{2ESR}} + i_{L2}\right] \\ \frac{di_{L2}}{dt} = \frac{1}{L_2}[-v_{batt} - i_{L2}L_{2ESR}] \\ \frac{di_{Lo}}{dt} = \frac{1}{L_o}[nv_{C1} - i_{Lo}L_{oESR} - i_{Co}C_{oESR} - v_{Co}] \\ \frac{dv_{Co}}{dt} = \frac{1}{C_o}i_{Co} = \frac{1}{C_o}\left[i_{Lo} - \frac{v_{Co}}{R_L+C_{oESR}}\right] \end{cases} \qquad (4)$$

This stage is the charging stage, and its state equations in this stage are presented in Eq. (5).

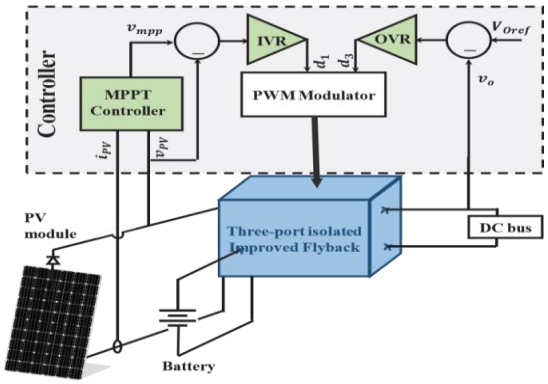

Fig 4.4.1.1 Closed loop controller of the proposed three-port converter

IJIREEICE

ISSN (Online) 2321-2004
ISSN (Print) 2321-5526

International Journal of Innovative Research in
Electrical, Electronics, Instrumentation and Control Engineering

Vol. 9, Issue 5, May 2021

DOI 10.17148/IJIREEICE.2021.9511

$$\begin{cases} \dfrac{dv_{C1}}{dt} = \dfrac{1}{C_1} i_{C1} = \dfrac{1}{C_1}[i_{PV} - i_{L2}] \\ \dfrac{dv_{C2}}{dt} = \dfrac{1}{C_2} i_{C2} = \dfrac{1}{C_2}\left[\dfrac{v_{batt} - v_{C2}}{C_{2_{ESR}}} + i_{L2}\right] \\ \dfrac{di_{L2}}{dt} = \dfrac{1}{L_2}\left[\begin{matrix} v_{C1} + i_{C1}C_{1_{ESR}} + \dfrac{v_{Co}}{n} + i_{Co}C_{o_{ESR}} \\ + i_{Lo}L_{o_{ESR}} - i_{L2}L_{2_{ESR}} - v_{batt} \end{matrix}\right] \\ \dfrac{di_{Lo}}{dt} = \dfrac{1}{L_o}[0] \\ \dfrac{dv_{co}}{dt} = \dfrac{1}{C_o} i_{Co} = \dfrac{1}{C_o}\left[i_{Lo} - \dfrac{v_{Co}}{R_L + C_{o_{ESR}}}\right] \end{cases} \quad (5)$$

By taking the average of the dynamic state equations in the three stages, the average state space model is derived using the traditional circuit averaging process.

The Control System Structure

To extract the maximum power from the PV module and to maintain a constant output voltage synchronously, a proper control design of the proposed multi-port converter is proposed in this section. Fig. 4.3.1.1 shows the block diagram of the control architecture connected to the proposed converter.

The output voltage regulator (OVR) takes the error in the output voltage of the multiport converter V_a as its input, and its output is the duty cycle d_3. The input voltage regulator (IVR) takes the error in the PV voltage where its reference voltage $V_{mpp}$is obtained from the MPPT controller, which based on P&O method, and its output is the duty cycle d_1.

The Small-Signal Model of the Proposed Converter

The small-signal value of the PV module current i_{PV} can be found by the first derivative of the current and voltage relationship as in Eq. (6).

$$i_{PV} = I_{SC} - I_S\left(e^{\frac{V_{PV}}{V_T}} - 1\right) \approx I_{SC} - I_S\, e^{\frac{V_{PV}}{V_T}} \quad (6)$$

I_{SC} is the short-circuit current, and I_S represents the reverse bias saturation current of the PV module, and V_T is the thermal voltage.

The first derivative for Eq. (6) is:

$$\frac{di_{PV}}{dt} = -\left(\frac{I_S}{V_T}\, e^{\frac{V_{PV}}{V_T}}\right)\frac{dv_{PV}}{dt} = -\left(\frac{1}{r_{PV}}\right)\frac{dv_{PV}}{dt}$$

$$\hat{\imath}_{PV} = -\frac{1}{r_{PV}} \cdot \hat{v}_{C1} \quad (7)$$

where r_{PV} represents the equivalent resistance of the PV module around a certain operating point specified by V_{C1}.

To this end, the small-signal model of the multi-port converter takes the following form:

$$\dot{\hat{x}}(t) = A\hat{x}(t) + B\hat{u}(t)$$

$$\hat{y}(t) = C\hat{x}(t)$$

where $\hat{x} = [\hat{v}_{C1} \quad \hat{v}_{C2} \quad \hat{\imath}_{L2} \quad \hat{\imath}_{Lo} \quad \hat{v}_{Co}]^T$, $u = [\hat{d}_1 \quad \hat{d}_3]^T$ is the vector of the control signals, and $\hat{y}(t) = [v_{C1}(t) \quad v_{Co}(t)]^T$. Then, the transfer function $G(s) = \frac{Y(s)}{U(s)} = C(sI - A)^{-1}B$, where $C = \begin{bmatrix} 1 & 0 & 0 & 0 & 0 \\ 0 & 0 & 0 & 0 & 1 \end{bmatrix}$, and I is the identity matrix. $G(s)$ can be expressed as follows:

$$G(s) = \begin{bmatrix} g_{11}(s) & g_{12}(s) \\ g_{21}(s) & g_{22}(s) \end{bmatrix} \quad (8)$$

IJIREEICE

ISSN (Online) 2321-2004
ISSN (Print) 2321-5526

International Journal of Innovative Research in
Electrical, Electronics, Instrumentation and Control Engineering

Vol. 9, Issue 5, May 2021

DOI 10.17148/IJIREEICE.2021.9511

Fig. 4.4.3.1 shows the signal flows of the plant and the controllers, the input voltage regulator ($G_{IVR}(s)$) and the output voltage regulator ($G_{OVR}(s)$). This MIMO plant has the coupling terms ◌ $g_{12}(s)$ and $g_{21}(s)$ depicted by Eq. (8). By proper design of the two controllers $G_{IVR}(s)$ and $G_{OVR}(s)$ and the decoupling terms, the input voltage V_{ic} and the output voltage V_{co} can be controlled separately.

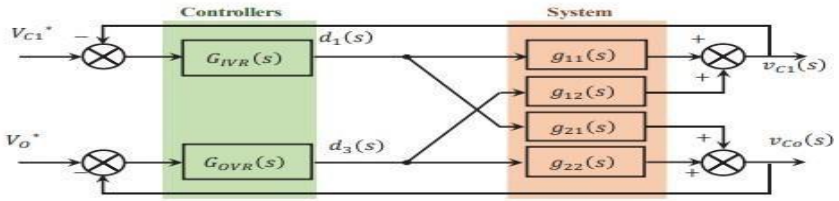

Fig 4.4.3.2. Signal flows of the plant and the controllers

The output voltage port has the highest priority over any other port requirement in any DC micro grid. Thus, the OVR loop is designed by one-decade higher bandwidth than that of IVR bandwidth. In other words, ◌ ଵ can be assumed to be constant when designing $G_{OVR}(s)$. Then the OVR is designed with the approximation that:

$$\frac{v_{Co}(s)}{d_3(s)} = g_{22}(s) \qquad (9)$$

Once $G_{OVR}(s)$ is designed, the decoupling model for $V_{ci}(s)$ / $d_1(s)$ can be derived as follows:

$$\frac{v_{C1}(s)}{d_1(s)} = g_{11}(s) - \frac{g_{21}(s)\, g_{12}(s)\, G_{OVR}(s)}{[1+g_{22}(s)\, G_{OVR}(s)]} \qquad (10)$$

5.RESULTS

MATLAB / Simulink is used to verify the proposed converter, build its controller, and to view its result. The values of the converter parameters used in the simulation are summarized in table 1.

TABLE I
THE VALUES OF THE PROPOSED MULTI-PORT CONVERTER PARAMETERS

PV maximum power point voltage	V_{mpp}	35.6 V	PV maximum power point current	I_{mpp}	9.79 A
Battery voltage	V_{batt}	30 V	Output voltage	V_o	100 V
PV module capacitor	C_1	110 μF	Battery module capacitor	C_2	100 μF
Output capacitor	C_o	220 μF	Magnetizing inductor	L_m	70 μH
Auxiliary inductor	L_2	0.86 mH	Output inductor	L_o	76 μH

A stable and high-bandwidth output-loop are preferable feature in the designing of the controller [24]. The open-loop transfer function of $V_{co}(s)$ / $d_3(s)$ is available from Eq. (9). The open-loop Bode plot of V_{co} (s) / $d_3(s)$ is shown in Fig.5.1.1.Therefore, a controller was designed to increase the system gain in the low-frequency region to eliminate the

IJIREEICE

ISSN (Online) 2321-2004
ISSN (Print) 2321-5526

International Journal of Innovative Research in
Electrical, Electronics, Instrumentation and Control Engineering

Vol. 9, Issue 5, May 2021

DOI 10.17148/IJIREEICE.2021.9511

steady-state error, and to maintain a sufficient phase margin. A 45° phase margin is the least commonly used criterion form stability point of view [26]. Thus, a classical PI controller will be able to handle these requirements. The crossover frequency for the OVR loop is set at 159.1 Hz with a phase margin of 68.3° and 25.6 dB gain margin which yields,

$$G_{OVR}(s) = 20.27\left(\frac{1 + 0.00095\,s}{s}\right)$$

The Bode plot of the system after the compensation is also shown in Fig. 5.1.1. After the OVR is designed, the IVR loop is designed based on Eq. (10). The Bode plot of $V_{ci}(s) / d_1(s)$ before and after compensation have been plotted in Fig.5.1.2. It shows that the lowfrequency region gains have been increased, and the crossover frequency is set at with phase margin 106° and ∞ inf gain margin which yields,

$$G_{IVR}(s) = 50\left(\frac{1 + 0.00059\,s}{s}\right)$$

These designed controllers are verified on the converter using MATLAB/Simulink under various situations. The results for step load change from 3A to 4A at t = 0.04 sec are shown in Fig. 9. The available PV power was insufficient to supply the load before and after the step load change. Each controller applied its objective although the available power from the PV module was insufficient. In Fig. 10, the converter supplies a constant load, but the available PV module power varies from sufficient to insufficient to view the battery contribution in balancing the output load voltage.

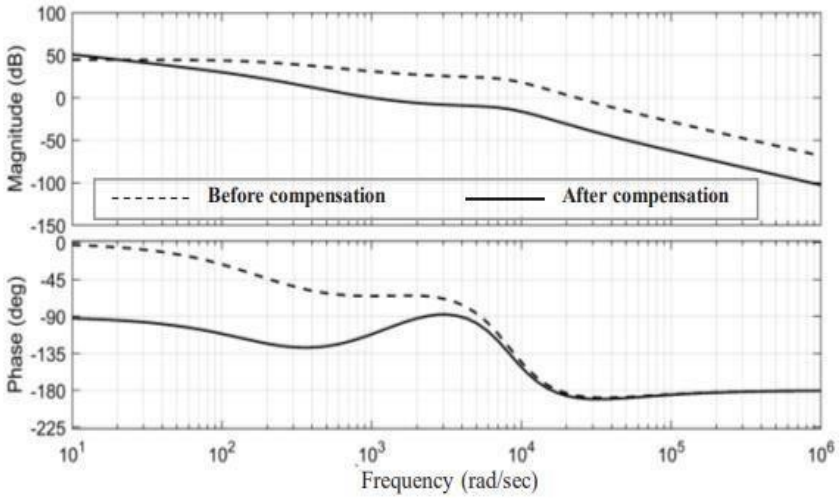

Fig 5.1.1 The output voltage control loop bode plot

The IVR tracks the reference maximum power point for the PV module even if it was a very low value as can be seen in Fig.5.1.4. The OVR maintain the required constant output voltage under any available PV power condition, while the battery provides the power balance in the system. The PV module power variation appears like disturbances to the system, thus the OVR should reject these disturbances and maintain a constant output voltage. The designed OVR prevent the output voltage variation from exceeding the ±5% of the desired output voltage, with short transient less than 6 ms and zero steady state error.

IJIREEICE

ISSN (Online) 2321-2004
ISSN (Print) 2321-5526

International Journal of Innovative Research in
Electrical, Electronics, Instrumentation and Control Engineering

Vol. 9, Issue 5, May 2021

DOI 10.17148/IJIREEICE.2021.9511

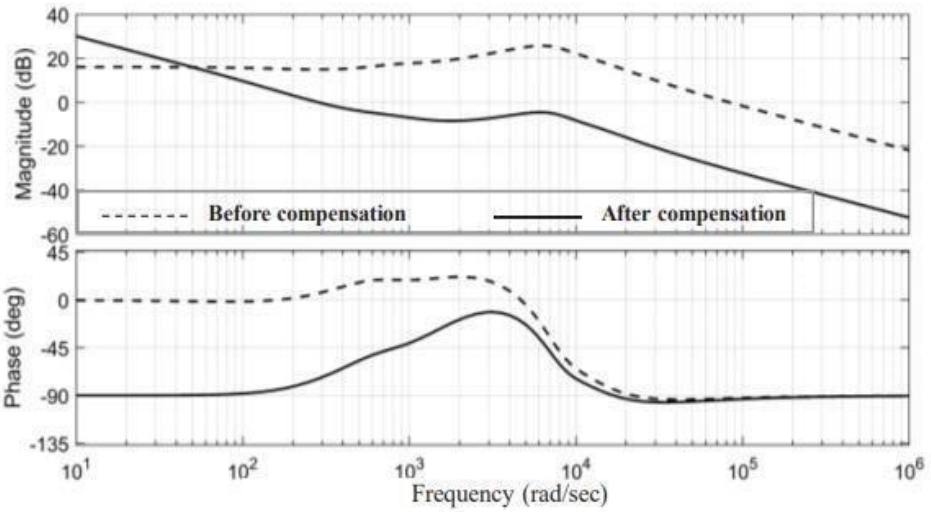

Fig 5.1.2 The input control loop bode plot

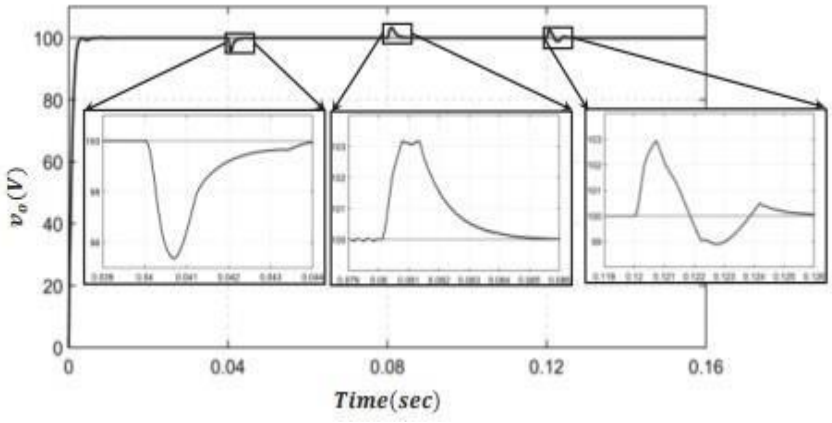

Figure 5.1.3. Zoom-in view of V_o, under the different mode of operations

Although the efficiency curve should be evaluated experimentally, the use of the parasitic elements for the passive elements and non-ideal switches in the proposed converter will reflect somehow the efficiency in our case. The efficiency curves of the proposed converter are shown in Fig. 5.1.5, for PV step-up and battery step-up modes. In case of the PV step-up, the converter has the highest efficiency to supply a 100W load by 93.5% efficiency, and in case of the battery step-up, the converter has the highest efficiency to supply a 100W load by 98% efficiency.

IJIREEICE

ISSN (Online) 2321-2004
ISSN (Print) 2321-5526

International Journal of Innovative Research in
Electrical, Electronics, Instrumentation and Control Engineering

Vol. 9, Issue 5, May 2021

DOI 10.17148/IJIREEICE.2021.9511

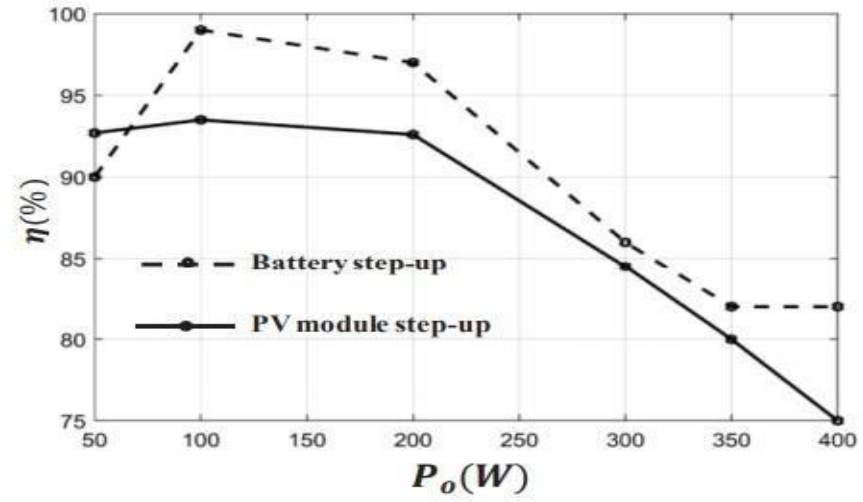

Figure 5.1.4. Efficiency curves of the proposed multi-port bi-directional

CONCLUSION

A multi-port isolated DC/DC converter was proposed with its modeling and control design. The output port is receiving its demand power without interruption while the power from the PV module is maximized. The battery stores the extra power when the power generated from the PV exceeds the load demand and supports the PV when the power generated from PV is insufficient. Moreover, synchronous rectification switches are used to improve the overall efficiency of the system. The converter is a modified Fly back converter that can provide two independent control signals, one control signal is used to track the maximum power point of the PV module and the other control signal is responsible to regulate the output voltage.

REFERENCES

[1] Huber, Laszlo, and Milan M. Jovanovic. "A design approach for server power supplies for networking applications." In APEC 2000. Fifteenth Annual IEEE Applied Power Electronics Conference and Exposition (Cat. No. 00CH37058), vol. 2, pp. 1163-1169.
IEEE, 2000.
[2] Zhao, Qun, Fengfeng Tao, and Fred C. Lee. "A front-end DC/DC converter for network server applications." In 2001 IEEE 32nd Annual Power Electronics Specialists Conference (IEEE Cat. No. 01CH37230), vol. 3, pp. 1535-1539. IEEE, 2001 [3] Xiaogang Feng, Jinjun Liu and F. Lee, "Impedance specifications for stable DC distributed power systems", IEEE Transactions on Power Electronics, vol. 17, no. 2, pp.
157-162, 2002.
[4] Zhao, Qun, and Fred C. Lee. "High performance coupled-inductor DCDC converters." In Proc. IEEE APEC, vol. 1, pp. 109-113. 2003.
[5] R. Wai and R. Duan, "High Step-Up Converter with CoupledInductor", IEEE Transactions on Power Electronics, vol. 20, no. 5, pp. 1025-1035, 2005.
[6] H. Tao, A. Kotsopoulos, J. Duarte and M. Hendrix, "Family of multiport bidirectional DC–DC converters", IEE Proceedings - Electric Power Applications, vol. 153, no. 3, p.
451, 2006.
[7] Ismail, Esam H., Mustafa A. Al-Saffar, and Ahmad J. Sabzali. "High conversion ratio
DC–DC converters with reduced switch stress." IEEE Transactions on Circuits and Systems I: Regular Papers 55, no. 7, pp. 2139-2151, 2008.
[8] Li, Wuhua, Xiaodong Lv, Yan Deng, Jun Liu, and Xiangning He. "A review of nonisolated high step-up DC/DC converters in renewable energy applications." In 2009 Twenty-Fourth Annual IEEE Applied Power Electronics Conference and Exposition, pp.
364-369. IEEE, 2009.
[9] Blaabjerg, Frede, Florin Iov, Tamas Kerekes, and Remus Teodorescu. "Trends in power electronics and control of renewable energy systems." In Proceedings of 14th International Power Electronics and Motion Control Conference EPE-PEMC 2010, pp. K-
1. IEEE, 2010.
[10] Chou, Hung-Ming. "Multi-port DC-DC Power Converter for Renewable Energy Application." PhD diss., Texas A & M University, 2010.